1780 © 1983 The Chemical Society of Japan Bull. Chem. Soc. Jpn., 56, 1780—1785 (1983) [Vol. 56, No. 6

An Interpretation of the Asymmetric Induction Observed in Rhodium-Bis(dibenzophosphole) Complex Catalyzed Hydroformylation According to an X-Ray Molecular Structure Analysis of an Iridium-(2*R*,3*R*)-2,3-*O*-Isopropylidene-1,4-bis(5*H*-dibenzophosphol-5-yl)-2,3-butanediol Complex

Teruyuki Hayashi,* Masato Tanaka, Ikuei Ogata, Teruyuki Kodama,†
Tamotsu Takahashi,† Yasuzo Uchida,† and Tokiko Uchida††
National Chemical Laboratory for Industry, Higashi, Yatabe, Tsukuba, Ibaraki 305
†*Department of Industrial Chemistry, Faculty of Engineering, The University of Tokyo, Hongo, Bunkyo-ku, Tokyo 113*
††*Department of Industrial Chemistry, Faculty of Science and Technology, Science University of Tokyo*
Higashikameyama, Yamazaki, Noda, Chiba 278

(Received April 3, 1982)

An X-ray molecular structure analysis of [(2*R*, 3*R*)-2,3-*O*-isopropylidene-1,4-bis(5*H*-dibenzophosphol-5-yl)-2,3-butanediol((−)-DIPHOL)](1,5-cyclooctadiene)chloroiridium(I) was carried out. The complex takes a distorted trigonal bipyramidal structure, and the chelate ring of (−)-DIPHOL makes a chair form, which decreases the distances of atoms in the chelate ring from the P–Ir–P coordination plane. Thus, the chiral coordination structure of DIPHOL becomes remarkably different from that of DIOP. Through a comparison of the results of X-ray analyses, the results obtained in asymmetric hydroformylation (predominant absolute configuration and optical yield of products) catalyzed by the rhodium-complexes were explained on the basis of some well-grounded assumptions.

X-Ray molecular structure analyses of presumed chiral complex catalysts have been studied in order to elucidate the mechanism of the asymmetric induction, especially in the asymmetric hydrogenation of prochiral olefins catalyzed by rhodium-optically active ligand-complexes.[1)] However, no attempt has yet been made in the field of symmetric hydroformylation, probably because the active catalyst species has not yet been made definite, as the reaction is a multistage one and proceeds under more severe conditions than in the case of hydrogenation, namely, at a higher reaction temperature and under a high carbon monoxide pressure.

A rhodium-catalyzed asymmetric hydroformylation reaction had been carried out by the use of chiral monophosphines[2,3)] and (2*R*,3*R*)-2,3-*O*-isopropylidene-1,4-bis(diphenylphosphino)-2,3-butanediol[(−)-DIOP][4–6)] as ligands. As the present authors reported previously, the enantioselectivity in rhodium-catalyzed asymmetric hydroformylation is considerably enhanced by the use of bis(5*H*-dibenzophosphole)s as chiral ligands in place of the corresponding bis(diphenylphosphine)s (Table 1).[7,8)] It was surprising that the prevailing absolute configurations of aldehydes obtained from styrene, 1-butene, and *cis*-2-butene by the use of (−)-DIPHOL or (1*R*,2*R*)-1,2-bis(5*H*-dibenzophosphol-5-ylmethyl)cyclobutane were the opposite of those obtained by the use of (−)-DIOP or (1*R*,2*R*)-1,2-bis(diphenylphosphinomethyl)cyclobutane respectively, though they have the same chiral backbone. An exception was observed in the case of *trans*-2-butene, from which the aldehyde with a very low optical yield was produced.

In the case of the rhodium–triphenylphosphine-complex catalyzed hydroformylation reaction, HRh-$(CO)_2PPh_3$ (in the dissociative mechanism) or HRh-$(CO)_2(PPh_3)_2$ (in the associative mechanism) is presumed as a key intermediate;[13)] only the former follows 18-electron rule upon coordination with a substrate. Similarly, when a bidentate ligand, (−)-DIOP, is used in place of PPh_3, the key intermediate is considered to have only one molecule of DIOP chelating as in HRh-(CO)[(−)-DIOP], which may well be supported by the following facts: 1) The optical yield in the hydroformylation of styrene was always higher than those obtained using C-chiral monophosphines,[10)] and 2) when the P/Rh atomic ratio in the system was increased, the optical yield levelled out at around the P/Rh value of 3.[14)] Therefore, the conformation of (+)-DIOP in an X-ray analysis of a pentacoordinated iridium complex

Table 1. Optical purity/% and prevailing absolute configuration of aldehydes formed in rhodium-catalyzed asymmetric hydroformylation

Substrate (Temp/°C)	Ligand			
	(2*R*,3*R*)-2, 3-*O*-Isopropylidene-1, 4-bis (phosphino)-2, 3-butanediols		(1*R*, 2*R*)-1,2-Bis-(phosphinomethyl)-cyclobutanes phosphino=	
	(−)-DIOP	(−)-DIPHOL	Ph_2P	DBP
Styrene (80)[a)]	12.3(*R*)	24.9(*S*)	2.8(*R*)	27.1(*S*)
1-Butene (90)	6.8(*R*)	16.2(*S*)	1.5(*R*)	16.2(*S*)
cis-2-Butene (120)	9.5(*S*)	16.6(*R*)	8.0(*S*)	16.8(*R*)
trans-2-Butene (120)	2.4(*S*)	2.3(*S*)	—	—

For the reaction conditions, see Ref. 8. The optical purities in Ref. 8 were recalculated on the basis of the value $[\alpha]_D = -238°$ of optically pure (−)-(*R*)-2-phenylpropanal; see Ref. 8.

—IrCl(COD)[(+)-DIOP] (**A**)[15,16]—is informative with regard to the conformation of (−)-DIOP in the catalytically active species.

The results in Table 1 seem to suggest that (−)-DIPHOL, upon coordination to rhodium, takes a chelate ring conformation essentially different from that of (−)-DIOP, which is a phenomenon caused by 5*H*-dibenzophospholyl (DBP) substitution for Ph_2P.

In order to compare the coordination structures of (−)-DIPHOL and (−)-DIOP, the present authors prepared IrCl(COD)[(−)-DIPHOL] (**B**) complex and determined its X-ray molecular structure. The mechanism of the asymmetric induction in the hydroformylation reaction will be described on the basis of both the structures.

Experimental

[(2*R*,3*R*)-2,3-*O*-Isopropylidene-1,4-bis(5*H*-dibenzophosphol-5-yl)-2,3-butanediol](1,5-cyclooctadiene)chloroiridium(I) (**B**) was prepared according to the procedure used for the corresponding (+)-DIOP complex.[15] Single crystals were obtained from the EtOH–toluene solution as yellow platelets. Found: C, 56.49; H, 4.89%. Calcd for $C_{39}H_{40}ClIrO_2P_2$: C, 56.41; H, 4.86%.

X-Ray Data Collection. A crystal with dimentions of 0.08×0.32×0.44 mm^3 was sealed in a glass capillary under a nitrogen atmosphere. After determining the preliminary data with the Weissenberg photographs, the unit-cell dimensions were refined by the least-squares procedure with the setting angle of 20 reflections ($26.0° < 2\theta < 34.3°$) on a Rigaku four circle diffractometer with LiF-monochromatized Mo *Kα* radiation (λ=0.71069 Å). Two sets of intensity data were measured in the θ-2θ scan mode: Data 1 with Mo *Kα* radiation, $2\theta \leq 60°$, λ=0.71069 Å; Data 2 with Co *Kα* radiation, $2\theta \leq 82°$, λ=1.5418 Å. In both cases, the θ scan width was ($1.2° + 0.45 \tan\theta$) with the scan rate of 2° min^{-1} (2θ). No significant changes were observed in the intensities of the four standard reflections monitored every 50 measurements throughout the data-collection. Lorentz and polarization corrections were usually applied, but no absorption correction was made. A total of 4075 reflections with $F_o > 3\sigma(F)$ in Data 1 were used in the subsequent calculations. The 1181 reflection pairs of $F_o(hkl)$ and $F_o(\bar{h}\bar{k}\bar{l})$ with $F_o > 3\sigma(F)$ of Data 2 were used only to confirm the absolute configuration, since the observed number was insufficient for the number of parameters to be refined, and the absorption correction was not taken into account.

Crystal Data: $IrClP_2O_2C_{39}H_{40}$, M_r=830.4, orthorhombic, space group $P2_12_12_1$, a=16.803(3), b=18.969(3), c=10.928(2) Å, V=3483.3(9) Å^3, Z=4, D_x=1.56 gcm^{-3}, μ(Mo *Kα*)=42.1 cm^{-1}, $F(000)$=1608, μ(Cu *Kα*)=90.2 cm^{-1}.

Structure Determination and Refinement. The structure was solved by the heavy-atom method and refined by the block-diagonal least-squares method. The quantity minimized was $\sum w(|F_o|-|F_c|)^2$, and the weight parameter was $(14.1/|F_o|)^2$ in the absolute scale. After several cycles with anisotropic non-hydrogen atoms, two enantiomorphic forms, one of which was made by inverting the atomic parameters of the other, were refined separately with anomalous dispersion correction. The *R* values of the forms were 0.087 and 0.093. Since the *R*-ratio, the number of observations, and the number of refined parameters were 1.16, 4075, and 407 respectively, the (2*S*,3*S*)-structure could be rejected at the 0.005 significance level.[17] To confirm the configuration, separate refinements with $F_o(hkl)$ and $F_o(\bar{h}\bar{k}\bar{l})$ were carried out with Data 2, which possessed a higher intensity (about four times) than Data 1. The *R* values and the *R* ratio were 0.082, 0.087, and 1.061 respectively, so the results agreed with those of Data 1. Table 2 compares the observed and calculated structure amplitudes between several Bijvoet pairs with Data 2.

The final refinement with Data 1 was calculated with anisotropic non-hydrogen atoms, anomalous dispersion corrections for Ir, Cl, and P atoms, and isotropic hydrogen atoms, which were geometrically located and which were given a constant temperature parameter of 4.5 Å^2. The final *R* and R_w values were 0.076 and 0.079 respectively. The maximun parameter shift to its e.s.d. ratio was less than 0.5. The atomic scattering factors and anomalous dispersion corrections for Ir, Cl, and P atoms were taken from the International Tables for X-ray Crystallography.[18] All the computations were carried out at the Computer Center of the University of Tokyo with the UNICS program system.[19] The final atomic coordinates are shown in Table 3.[20]

Results

Some selected bond distances and angles of **B** are given in Table 4. An ORTEP[21] drawing and the numbering of the atoms are shown in Fig. 1. The Ir–Cl distance (2.549 Å) is fairly large in comparison with those in IrCl(CO)(P-*o*-Tol_3)$_2$[22] (2.43 Å) and in IrCl(CO)$_2$-

TABLE 2. OBSERVED AND CALCULATED STRUCTURE AMPLITUDES OF SEVERAL BIJVOET PAIRS

h	k	l	$F_O(hkl)$	$F_O(\bar{h}\bar{k}\bar{l})$	$F_C(hkl)$	$F_C(\bar{h}\bar{k}\bar{l})$	$\frac{F_O(hkl)}{F_O(\bar{h}\bar{k}\bar{l})}$	$\frac{F_C(hkl)}{F_C(\bar{h}\bar{k}\bar{l})}$
4	2	1	43	54	42	54	0.80	0.78
1	1	2	180	160	151	136	1.13	1.11
2	6	2	85	69	83	70	1.23	1.19
5	4	2	49	27	48	25	1.81	1.92
5	6	2	57	45	54	46	1.27	1.17
1	10	3	26	37	32	37	0.70	0.86
7	9	3	61	50	60	50	1.22	1.20
8	4	4	50	40	51	41	1.25	1.24
6	10	5	70	63	70	67	1.11	1.04
3	3	6	49	40	42	32	1.23	1.31
4	5	6	68	58	67	60	1.17	1.12
4	7	6	52	44	53	42	1.18	1.26

Table 3. The positional parameters and equivalent isotropic temperature parameters, with their estimated standard deviations in parentheses

$B_{eq}=4/3\sum_i a_i^2\beta_{ii}$

Atom	x	y	z	B_{eq}/Å
Ir	0.07606(4)	0.16927(4)	0.22104(7)	2.32(1)
Cl	0.2259(3)	0.1579(4)	0.2517(5)	4.4(2)
P(1)	0.1118(3)	0.1990(3)	0.0243(5)	2.6(1)
P(2)	0.0660(3)	0.2831(3)	0.2941(4)	2.4(1)
O(1)	0.248(1)	0.3737(9)	−0.028(2)	4.2(5)
O(2)	0.204(1)	0.436(1)	0.136(2)	5.1(5)
C(01)	0.195(1)	0.2586(9)	−0.005(2)	2.5(5)
C(02)	0.182(1)	0.334(1)	0.016(2)	3.1(5)
C(03)	0.097(1)	0.363(1)	0.208(2)	2.9(5)
C(04)	0.181(1)	0.363(1)	0.149(2)	3.3(5)
C(05)	0.253(2)	0.442(1)	0.033(2)	4.4(7)
C(06)	0.226(2)	0.501(2)	−0.045(3)	7(1)
C(07)	0.342(2)	0.451(2)	0.078(4)	8(1)
C(11)	0.034(1)	0.225(1)	−0.084(2)	3.1(5)
C(12)	−0.022(1)	0.278(2)	−0.066(2)	4.5(7)
C(13)	−0.084(2)	0.282(2)	−0.160(3)	5.2(8)
C(14)	−0.088(2)	0.242(2)	−0.259(3)	6.4(9)
C(15)	−0.035(2)	0.191(2)	−0.262(3)	7(1)
C(16)	0.032(2)	0.178(2)	−0.183(2)	5.7(9)
C(21)	0.140(1)	0.122(1)	−0.073(2)	3.2(5)
C(22)	0.201(2)	0.073(1)	−0.055(3)	5.1(8)
C(23)	0.213(2)	0.021(1)	−0.147(3)	5.1(8)
C(24)	0.166(2)	0.019(1)	−0.247(3)	6(1)
C(25)	0.106(2)	0.067(2)	−0.265(3)	6.1(9)
C(26)	0.093(2)	0.122(1)	−0.178(2)	4.2(7)
C(31)	0.104(1)	0.304(1)	0.446(2)	3.3(5)
C(32)	0.182(1)	0.290(1)	0.488(2)	4.6(7)
C(33)	0.198(2)	0.314(2)	0.610(3)	5.2(8)
C(34)	0.144(2)	0.352(2)	0.677(3)	5.5(9)
C(35)	0.068(2)	0.362(1)	0.635(2)	4.9(7)
C(36)	0.047(1)	0.337(1)	0.518(2)	2.2(5)
C(41)	−0.034(1)	0.315(1)	0.337(2)	3.0(5)
C(42)	−0.101(1)	0.316(1)	0.268(2)	3.9(6)
C(43)	−0.172(1)	0.342(2)	0.320(2)	4.8(7)
C(44)	−0.172(2)	0.370(2)	0.441(3)	5.3(8)
C(45)	−0.102(1)	0.372(2)	0.510(2)	4.7(7)
C(46)	−0.031(1)	0.342(1)	0.458(2)	3.0(5)
C(1)	−0.027(2)	0.117(2)	0.168(3)	5.4(8)
C(2)	0.031(2)	0.071(2)	0.152(3)	6.0(9)
C(3)	0.042(3)	0.010(2)	0.238(6)	4(1)
C(4)	0.054(3)	0.020(2)	0.351(5)	4(1)
C(5)	0.075(2)	0.094(2)	0.382(3)	6.4(9)
C(6)	0.015(2)	0.146(1)	0.405(2)	3.6(7)
C(7)	−0.072(2)	0.129(2)	0.389(3)	6.7(9)
C(8)	−0.097(1)	0.112(2)	0.258(2)	5.3(8)

(PPh$_3$)$_2$[23] (2.37 Å), while it is similar to that in **A** (2.599 Å).[15] The Ir–P distances (2.303 Å/2.310 Å) are similar not only to those in **A** (2.327 Å/2.339 Å),[15] but also to those in IrCl(CO)(PMePh$_2$)$_2$[24] (2.342 Å/2.320 Å), IrCl(CO)$_2$(PPh$_3$)$_2$[23] (2.341 Å/2.322 Å), and IrMe(COD)**P**$_2$ (**P**$_2$=2PPhMe$_2$,[25] DPPE,[26] and DPPP[27]) (2.316 Å/2.329 Å, 2.309 Å/2.337 Å, 2.308 Å/2.308 Å). The Ir–(C=C) distances are 2.02 Å for C(1/2) and 2.19 Å for C(5/6), similar to those in IrMe(COD)**P**$_2$ (2.078 Å/2.117 Å, 2.033 Å/2.127 Å, 2.011 Å/2.106 Å). C(1/2) and C(5/6) represent the midpoints of the C(1)=C(2) and C(5)=C(6) double bonds. Regarding the DIPHOL ligand, the P–C, C–C, and C–O distances in the chelate ring and in the dioxolane ring are similar to those in DIOP complexes–**A**, HRh[(+)-DIOP]$_2$,[28] and HRuCl-[(+)-DIOP]$_2$.[29] The bond distances and angles in the DBP moieties are reasonable in comparison with those in dibenzophosphole complexes, Ni(CN)$_2$(DBP-R)$_3$ (R=Me and Et),[30] NiBr$_2$(DBP-Me)$_2$.[31] The distances of the C–C and C=C bonds in the COD ligand are 1.40—1.53 Å for sp^3–sp^3 and sp^2–sp^3 bonds and 1.31—1.38 Å for sp^2–sp^2 bonds, which are comparable with

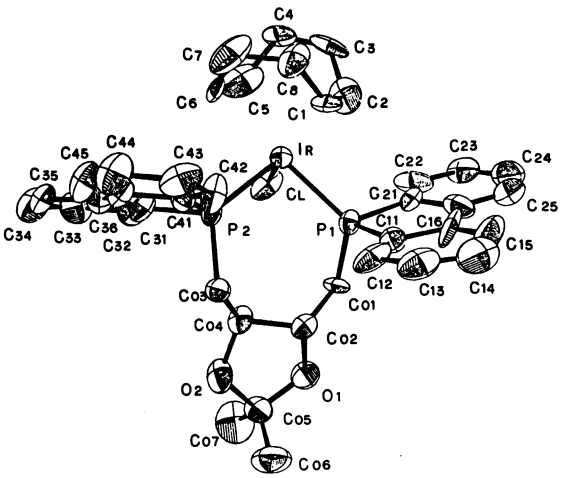

Fig. 1. An ORTEP drawing of IrCl(1,5-COD)[(−)-DIPHOL] (**B**).

the values in IrMe(COD)$\mathbf{P}_2$.[25–27]

The coordination structure around the Ir atom is regarded as a distorted trigonal bipyramid with P(1) and C(5/6) in apical positions, according to the following results: 1) The ∠P(1)IrCl, ∠P(1)IrP(2), and ∠P(1)-IrC(1/2) angles are between 83.4—96.5°, and ∠C(5/6)-IrC(1/2), ∠C(5/6)IrCl, and ∠C(5/6)IrP(2) are between 82.1—94.7°, while ∠P(1)IrC(5/6)=168.5°. 2) The distance of Ir–C(1/2) is smaller than that of Ir–C(5/6). In all trigonal bipyramidal IrMe(COD)$\mathbf{P}_2$ complexes,[25–27] the distances of the equatorial C=C from Ir are shorter than those of the apical one (2.01—2.08 Å/2.11, 2.13 Å). 3) The dihedral angles between the faces of the polyhedron which cross at Cl–C(1/2), C(1/2)–P(2), and P(2)–Cl are 38.9°, 44.1°, and 75.7° respectively. As has been pointed out by Muetterties and Guggenberger,[32] the three smaller angles in the ideal trigonal bipyramid are all 53.1°, while those in the ideal square pyramid are 0.0°, 75.7°, and 75.7°. The comparison of the sum of the squares of each deviation in the angles indicated that the structure of the polyhedron of **B** is nearly trigonal bipyramidal.

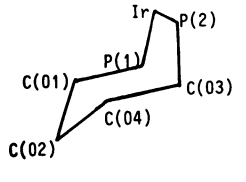

The chelate ring makes a chair form with an almost flat "back" which consists of P(1)–Ir–P(2)–C(03) and a "foot" which consists of C(02). As a result of this chair-form conformation, the dihedral angles between the P(1)–Ir–P(2) plane and the two DBP moieties represented by C(11)–P(1)–C(21) and C(31)–P(2)–C(41) are 60.4° and 82.5° respectively. That is, the DBP moiety containing P(2) is almost perpendicular to the P(1)–Ir–P(2) plane, while that containing P(1) is skewed.

The molecular structures of **A**[15] and **B** are presented in Fig. 2 so that each Cl–P(1)–Ir–P(2) structure takes a similar direction. **A** has (+)-DIOP as the ligand, while the hydroformylation reactions in Table 1 were

TABLE 4. BOND LENGHTS AND BOND ANGLES OF IrCl (1,5-COD)[(−)-DIPHOL](**B**)

Bond length	l/Å		l/Å
Ir–Cl	2.550(7)	Ir–C(1)	2.09(3)
Ir–P(1)	2.302(6)	Ir–C(2)	2.15(3)
Ir–P(2)	2.308(5)	Ir–C(5)	2.27(3)
DIPHOL ligand		Ir–C(6)	2.31(3)
P(1)–C(01)	1.83(2)	COD ligand	
P(1)–C(11)	1.83(2)	C(1)–C(2)	1.31(5)
P(1)–C(21)	1.87(2)	C(2)–C(3)	1.51(7)
P(2)–C(03)	1.86(2)	C(3)–C(4)	1.27(8)
P(2)–C(31)	1.82(2)	C(4)–C(5)	1.48(6)
P(2)–C(41)	1.84(2)	C(5)–C(6)	1.43(4)
C(01)–C(02)	1.46(3)	C(6)–C(7)	1.49(5)
C(02)–O(1)	1.44(3)	C(7)–C(8)	1.53(5)
C(03)–C(04)	1.55(3)	C(8)–C(1)	1.52(4)
C(04)–O(2)	1.45(3)	Ir–C(1/2)	2.02
C(02)–C(04)	1.56(4)	Ir–C(5/6)	2.19
O(1)–C(05)	1.46(3)	Av. of C–C bonds in benzene rings	
O(2)–C(05)	1.41(3)		
C(05)–C(06)	1.48(5)	Ring 1	1.39
C(05)–C(07)	1.57(5)	Ring 2	1.39
C(16)–C(26)	1.48(5)	Ring 3	1.40
C(36)–C(46)	1.47(3)	Ring 4	1.41
Bond angle	**θ/°**		**θ/°**
Cl–Ir–P(1)	83.5(2)	Cl–Ir–C(1/2)	127
Cl–Ir–P(2)	96.1(2)	Cl–Ir–C(5/6)	93
P(1)–Ir–P(2)	96.5(2)	P(1)–Ir–C(1/2)	92
C(1)–Ir–C(5)	84(1)	P(1)–Ir–C(5/6)	169
C(1)–Ir–C(6)	77(1)	P(2)–Ir–C(1/2)	137
C(2)–Ir–C(5)	74(1)	P(2)–Ir–C(5/6)	95
C(2)–Ir–C(6)	89(1)	COD ligand	
DIPHOL ligand		C(1)–C(2)–C(3)	121(4)
Ir–P(1)–C(01)	121.1(8)	C(2)–C(3)–C(4)	120(5)
Ir–P(2)–C(03)	124.8(7)	C(3)–C(4)–C(5)	114(5)
Ir–P(1)–C(11)	118.8(7)	C(4)–C(5)–C(6)	122(3)
Ir–P(1)–C(21)	113.8(8)	C(5)–C(6)–C(7)	121(3)
Ir–P(2)–C(31)	119.4(8)	C(6)–C(7)–C(8)	115(3)
Ir–P(2)–C(41)	117.4(7)	C(7)–C(8)–C(1)	112(3)
C(01)–P(1)–C(11)	105(1)	C(8)–C(1)–C(2)	128(3)
C(01)–P(1)–C(21)	101(1)		
C(11)–P(1)–C(21)	92(1)		
C(03)–P(2)–C(31)	100(1)	C(1/2)–Ir–C(5/6)	82
C(03)–P(2)–C(41)	97(1)		
C(31)–P(2)–C(41)	91(1)		
P(1)–C(01)–C(02)	117(2)	DIPHOL ligand	
C(01)–C(02)–O(1)	110(2)	C(11)–C(16)–C(26)	115(3)
C(01)–C(02)–C(04)	120(2)	C(21)–C(26)–C(16)	115(3)
O(1)–C(02)–C(04)	98(2)	C(31)–C(36)–C(46)	113(2)
C(02)–O(1)–C(05)	111(2)	C(41)–C(46)–C(36)	115(2)
P(2)–C(03)–C(04)	117(2)	Av. of angles in each benzene ring	
C(03)–C(04)–O(2)	106(2)		
C(03)–C(04)–C(02)	114(2)		120
O(2)–C(04)–C(02)	104(2)		
C(04)–O(2)–C(05)	109(2)		
O(1)–C(05)–O(2)	105(2)		
O(1)–C(05)–C(06)	113(2)		
O(1)–C(05)–C(07)	107(2)		
O(2)–C(05)–C(06)	110(2)		
O(2)–C(05)–C(07)	108(2)		

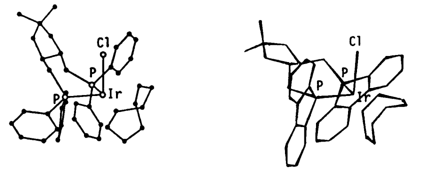

IrCl(COD)[(+)-DIOP] (A)
S. Brunie, J. Mazan, N. Langlois, and H. B. Kagan, *J. Organomet. Chem.*, 114, 225 (1976). (Ref. 15)

IrCl(COD)[(-)-DIPHOL] (B)
in this work

Fig. 2. X-Ray molecular structures of IrCl(1,5-COD)-chiral diphosphine complexes.

carried out by the use of (−)-DIOP and (−)-DIPHOL, with (2*R*,3*R*)-chirality in the backbones. The chelate-ring conformation in **A**[16] takes a skewed chair form[33,34] with a skewed "back" which consists of CH_2–P–Ir–P and with a "foot" which consists of *t*-CH in DIOP. The displacements of fluxional Ph_2P groups in **A** by rigid DBP groups must increase the steric repulsion between aromatic groups; this may well be removed by a slight distortion of the chelate-ring conformation from the skewed chair form to the chair form described above. Thus, the dihedral angle between the C(03)–P(2)–Ir and P(2)–Ir–P(1) planes, which is 30.0° in **A**,[16] is reduced to 8.4° in **B**. Consequently, C(03)–P(2)–Ir–P(1)–C(21) makes an approximate plane, since a dihedral angle between the P(2)–Ir–P(1) and Ir–P(1)–C(21) planes is also small in **B** (7.2°). These conformational distortions of the chelate ring caused a fairly large difference in the structure of the complex; that is, the distance from the quart-C in the dioxolane ring to the P(1)–Ir–P(2) plane is reduced from 3.98 Å in **A** to 2.22 Å in **B**. Therefore, the mode of the protrusion of aromatic rings of the diphosphines into the coordination site for substrates or reactants, *i.e.*, the steric environment in the site, is profoundly changed, as will be shown below.

Discussion

Although the mechanism of asymmetric induction in hydroformylation has not yet been established, the difference between the stability of the diastereomeric intermediates, the hydridorhodium–(carbonyl)–(π-olefin)–diphosphine complexes, must play a part in the determination of the chirality of products. This is why the three kinds of butenes—1-butene, *cis*-2-butene, and *trans*-2-butene—all of which must go through the same *s*-butyl intermediate to be transformed to optically active 2-methylbutanal, gave aldehydes of different chiralities and different optical yields. (Table 1) The results in Table 1 can be explained on the basis of the molecular structures of **A** and **B** according to the following well-grounded assumptions: 1) The coordination structures of diphosphines in the diastereomeric rhodium–(π-olefin)–intermediate complexes are the same as in the iridium complexes, **A** and **B** respectively. 2) The coordination structures around the rhodium atom in the intermediate complexes are trigonal bipyramidal. 3) H and CO occupy apical positions. 4) The bulkier ligands, a chelating diphosphine and π-olefin, occupy equatorial positions, with angles of about 120° to each other, in order to release the steric congestions. If one of the three bulky ligands happens to occupy an apical position, it must have an angle of 90° with one of the other two in the equatorial position. Assumptions 2—4) can be explained by the X-ray molecular structure of $HRh(CO)(PPh_3)_3$,[35] which has a trigonal bipyramidal structure with H and CO in the apical positions and with three bulkier PPh_3's in the equatorial positions. 5) H in the rhodium intermediate complexes occupies the position of Cl in **A** and **B**; that is, the smallest ligand occupies the same side as the chelating diphosphine with regard to the P–Ir–P plane. This last assumption is acceptable if one considers the steric repulsion between the said apical position and the bridgehead CH or methylene CH_2 in the chelate ring.[36] This repulsion in the DIOP complex may be reduced to some extent in the DIPHOL complex, because the atoms comprising the chelate ring are placed nearer to the P–Ir–P plane, that is, farther from the apical H ligand, in the DIPHOL complex than in the DIOP complex.

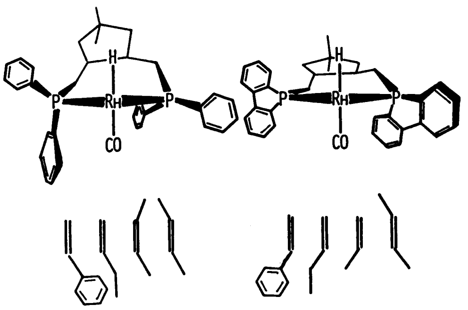

Fig. 3. Schematic coordination structures and conceivable modes of olefin π-coordination.

In view of the above considerations, the steric environment of the two complexes is considered to be as is schematically drawn in Fig. 3, viewed from the coordination site of π-olefin. Although the difference in the conformations of the chelate rings is small between DIOP and DIPHOL complexes, the steric environment around the π-olefin coordination site is greatly changed, as one can recognize from Fig. 2 and, more directly, from Fig. 3.

As the present X-ray analysis shows, the chelate ring of (−)-DIPHOL is closer to the P–Ir–P coordination plane than is that of (−)-DIOP. Consequently, in the (−)-DIPHOL complex, the plane of the left DBP group becomes perpendicular to the P–Ir–P plane and parallel to the π-olefin coordination site, while the right DBP group protrudes into the middle of the π-olefin coordination site, as if it were a large wing.

In contrast with the case of the asymmetric hydrogenation of enamides or dehydroamino acid derivatives, the substrate olefins in Table 1 have no functional group which can exert an attractive interaction with the rhodium center or other part of the complex. The high reaction temperature and pressure are also disadvantageous to such an interaction. Therefore, the coordination structure of the substrates must be controlled by the steric repulsion only. In addition, olefins need to π-coordinate to the rhodium atom with the substituents downward (the opposite side to hydrido with regard to the P–Ir–P plane) in order to be transformed into optically active branched aldehydes. Thus, the substrates prefer to π-coordinate to the rhodium center of the (−)-DIPHOL complex as is shown in Fig. 3. (Superimpose the double bonds of the substrates on the rhodium center.)

On the other hand, in the Rh–(−)-DIOP complex, the free rotation of the lower-left phenyl group is restricted by the other phenyl groups, and the steric hindrance by the *ortho*-CH in the coordination site for olefins seems to be significant. Therefore, the substrates prefer to π-coordinate to Rh–(−)-DIOP as is shown in Fig. 3, which leads to the prevailing configuration of products being the opposite of those when Rh–(−)-DIPHOL is used. However, since the upper-right phenyl group is parallel to, but also protrudes into the π-olefin coordination site, the chiral environment around the coordination site for substrates must be less selective. Consequently, the optical yields of products formed by the use of (−)-DIPHOL as a chiral ligand are higher than those formed by the use of (−)-DIOP. Thus, the results in Table 1 can be explained.

The authors wish to express their hearty thanks to Professor H. B. Kagan for sending them his detailed data on the X-ray molecular structure analysis of IrCl(COD)[(+)-DIOP] and for permitting them to reproduce the figure of Ref. 15. They also appreciate very much the permission for the reproduction given by Elsevier Sequoia S. A.

References

1) W. S. Knowles, B. D. Vineyard, M. J. Sabacky, and B. R. Stults, in "Fundamental Research in Homogeneous Catalysis," ed by M. Tsutsui, Plenum, New York (1979), Vol. 3, pp. 537—548.

2) M. Tanaka, Y. Watanabe, T. Mitsudo, K. Yamamoto, and Y. Takegami, *Chem. Lett.*, **1972**, 483.

3) I. Ogata and Y. Ikeda, *Chem. Lett.*, **1972**, 487.

4) C. Salomon, G. Consiglio, C. Botteghi, and P. Pino, *Chimia*, **27**, 215 (1973).

5) G. Consiglio, C. Botteghi, C. Salomon, and P. Pino, *Angew. Chem., Int. Ed. Engl.*, **12**, 669 (1973).

6) R. Stern, A. Hirschauer, and L. Sajus, *Tetrahedron Lett.*, **1973**, 3247.

7) M. Tanaka, Y. Ikeda, and I. Ogata, *Chem. Lett.*, **1975**. 1115.

8) T. Hayashi, M. Tanaka, Y. Ikeda, and I. Ogata, *Bull. Chem. Soc. Jpn.*, **52**, 2605 (1979). When these studies (Refs. 7 and 8) were carried out, the $[\alpha]_D$ value of optically pure 2-phenylpropanal had been claimed in Ref. 9 to be 238°; this value had been indirectly evaluated by extrapolation. The authors of Refs. 7 and 8 adopted the value of 160°,$^{10)}$ evaluated through the reduction to 2-phenylpropanol. However, in 1982, the value of 238° was directly confirmed as in Refs. 11 and 12, and so the present authors adopt this value in this paper.

9) C. Botteghi, G. Consiglio, and P. Pino, *Justus Liebigs Ann. Chem.*, **1974**, 864.

10) M. Tanaka, Y. Watanabe, T. Mitsudo, and Y. Takegami, *Bull. Chem. Soc. Jpn.*, **47**, 1698 (1974).

11) T. Hayashi, M. Konishi, M. Fukushima, T. Mise, M. Kagotani, M. Tajika, and M. Kumada, *J. Am. Chem. Soc.*, **104**, 180 (1982).

12) C. U. Pittman, Jr., Y. Kawabata, and L. Flowers. *J. Chem. Soc., Chem. Commun.*, **1982**, 473.

13) C. K. Brown and G. Wilkinson, *J. Chem. Soc., A*, **1970**, 2753.

14) M. Tanaka, unpublished results.

15) S. Brunie, J. Mazan, N. Langlois, and H. B. Kagan, *J. Organomet. Chem.*, **114**, 225 (1976).

16) H. B. Kagan, private communication (1980).

17) W. C. Hamilton, *Acta Crystallogr.*, **18**, 502 (1965).

18) "International Tables for X-ray Crystallography," Kynoch, Birmingham (1974), Vol. 4.

19) "UNICS. The Universal Crystallographic Computing System," ed by T. Sakurai, The Crystallographic Society of Japan, Tokyo (1967).

20) Lists of structure factors and anisotropic thermal parameters have been deposited at the office of the Chemical Society of Japan as Document No. 8317.

21) C. K. Johnson, ORTEP. Report ORNL-3794. Oak Ridge National Laboratory, Tennessee (1965).

22) R. Brady, W. H. de Camp, B. R. Flynn, M. L. Schneider J. D. Scott, L. Vaska, and M. F. Werneke, *Inorg. Chem.*, **14**, 2669 (1975).

23) N. C. Payne and J. A. Ibers, *Inorg. Chem.*, **8**, 2714 (1969).

24) J.-Y. Chen, J. Halpern, and J. Molin-Case, *J. Coord. Chem.*, **2**, 239 (1973).

25) M. R. Churchill and S. A. Bezman, *Inorg. Chem.*, **11**, 2243 (1972).

26) M. R. Churchill and S. A. Bezman, *Inorg. Chem.*, **12**, 260 (1973).

27) M. R. Churchill and S. A. Bezman, *Inorg. Chem.*, **12**, 531 (1973).

28) R. G. Ball, B. R. James, D. Mahajan, and J. Trotter, *Inorg. Chem.*, **20**, 254 (1981).

29) R. G. Ball and J. Trotter, *Inorg. Chem.*, **20**, 261 (1981).

30) H. M. Powell, D. J. Watkin, and J. B. Wilford, *J. Chem. Soc., A*, **1971**, 1803.

31) D. J. Watkin, *J. Chem. Soc., Dalton Trans.*, **1976**, 1803.

32) E. L. Muetterties and L. J. Guggenberger, *J. Am. Chem. Soc.*, **96**, 1748 (1974).

33) D. F. Bocian, H. M. Pickett, T. C. Rounds, and H. L. Strauss, *J. Am. Chem. Soc.*, **97**, 687 (1975).

34) W. M. J. Flapper and C. Romers, *Tetrahedron*, **31**, 1705 (1975).

35) S. J. LaPlaca and J. A. Ibers, *J. Am. Chem. Soc.*, **85**, 3501 (1963).

36) R. Graser, *Tetrahedron Lett.*, **1975**, 2127.